CD47 promotes T-cell lymphoma metastasis by upregulating AKAP13-mediated RhoA activation

Yuichi Kitai[1]*, Marie Ishiura[1], Kodai Saitoh[1], Naoki Matsumoto[1], Kimiya Owashi[1], Shunsuke Yamada[1], Ryuta Muromoto[1], Jun-ichi Kashiwakura[1], Kenji Oritani[2] and Tadashi Matsuda[1]**

1 Department of Immunology, Graduate School of Pharmaceutical Sciences, Hokkaido University, Kita 12, Nishi 6, Kita-Ku, Sapporo, Hokkaido 060-0812, Japan
2 Department of Hematology, International University of Health and Welfare, Narita, Chiba 286-8686, Japan.

* Corresponding author: Dr. Yuichi Kitai
E-mail: yu-kitai@pharm.hokudai.ac.jp

* *Corresponding author: Prof. Tadashi Matsuda
E-mail: tmatsuda@pharm.hokudai.ac.jp
Running title: CD47 promotes T-cell lymphoma metastasis

Keywords: integrin, phagocytosis, Rho-GEF, small-G protein, TSP-1

Abstract

CD47, a 50 kDa transmembrane protein, facilitates integrin-mediated cell adhesion and inhibits cell engulfment by phagocytes. Since CD47 blocking promotes engulfment of cancer cells by macrophages, it is important to clarify the mechanism of CD47 signaling in order to develop treatments for diseases involving CD47-overexpressing cancer cells, including breast cancer and lymphoma. Here, we show that CD47 plays an essential role in T-cell lymphoma metastasis by upregulating basal RhoA activity independent of its anti-phagocytic function. CD47 interacts with AKAP13, a RhoA-specific guanine nucleotide exchange factor (GEF), and facilitates AKAP13-mediated RhoA activation. Our study shows that CD47 has a novel function on the AKAP13-RhoA axis and suggests that CD47-AKAP13 interaction would be a novel target for T-cell lymphoma treatment.

Introduction

Lymphoma is a malignancy of immature or mature lymphocytes and is divided into several subtypes according to its origin and morphology. Among them, T-cell lymphoma is a rare malignancy and a subtype of non-Hodgkin lymphoma; T-cell lymphoma includes T-lymphoblastic lymphoma and peripheral T-cell lymphoma. Patients with T-cell malignancy generally receive anticancer chemotherapy, but if the lymphoma becomes refractory to chemotherapy, the prognosis is poor (1). Therefore, it is important to identify the molecules that correlate with T-cell lymphoma exacerbation and the mechanism by which T-cell lymphoma overcomes chemoresistance.

CD47, one of the cell surface transmembrane proteins, was originally identified as an integrin-associated protein and correlated with cell adhesion and migration (2). CD47 binds to thrombospondin-1 (TSP-1), an extracellular matrix protein, and then activates RhoA- and Rac1-mediated signaling. These small G proteins contribute to cell proliferation, morphology and cancer metastasis (3). RhoA and Rac1 are activated by their binding to GTP, which is promoted by guanine nucleotide exchange factor (GEF), and deactivated by hydrolysis of the GTP with GTPase-activating protein (GAP). Many GEFs and GAPs have been identified, and a previous study showed that an inhibitor of RhoA GEFs decreased cancer cell proliferation and invasion (4). Thus, CD47 inhibition has the potential to decrease RhoA activity, resulting in the suppression of cancer proliferation and metastasis.

A recent study showed that CD47 binds to SIRPα in phagocytes and inhibits phagocytosis, which is a pathway called “Don’t eat me signaling”. Certain types of cancer cells, including non-Hodgkin lymphoma, acute myeloid lymphoma and breast cancer, overexpress CD47 and escape from its engulfment by phagocytes (5). CD47 neutralizing antibody promotes engulfment of cancer cells by macrophages and activates antitumor immune responses, and its clinical trials for lymphoma therapy are currently ongoing (6). Under these circumstances, elucidation of the mechanism of CD47 signaling would contribute to the development of a novel lymphoma treatment strategy.

Here we show that CD47 plays an essential role in T-cell lymphoma metastasis by upregulating basal RhoA activity but not basal Rac1 activity. The cytosolic domain of CD47 interacts with AKAP13, one of the RhoA-specific GEFs, and activates AKAP13-mediated RhoA. The phagocytic efficiency of CD47-deficient EG7 cells by phagocytes was comparable with that of wild-type EG7 cells, indicating that CD47-mediated RhoA regulation makes a greater contribution to T-cell lymphoma metastasis than the anti-phagocytic function of CD47. Our study provides new insight into the function of CD47 on the AKAP13-RhoA axis and accentuates the importance of CD47-targeted drug development for T-cell lymphoma treatment.

Materials and methods

Animals

All animals were kept under specific pathogen-free conditions. C57BL/6 and BALB/c mice were purchased from Sankyo Labo Service Corporation. All animal experiments were performed with the approval of the Animal Research Committee of Hokkaido University.

Reagents and cells

HeLa and HEK293T cells were cultured in Dulbecco's modified Eagle's medium (DMEM; Sigma-Aldrich Co., MO) supplemented with 10% fetal bovine serum (FBS; Gibco, MA) and 0.05 mM 2-mercaptoethanol (Nacalai Tesque, Inc., Kyoto, Japan) at 37°C in a humidified 5% CO_2/95% air atmosphere. EG7 cells and L5178Y cells were cultured in RPMI 1640 medium (Sigma-Aldrich) supplemented with 10% FBS and 0.05 mM 2-mercaptoethanol. E0771 cells, a mouse breast adenocarcinoma cell line, were purchased from CH3 BioSystems (NY). LLC, a mouse Lewis lung carcinoma cell line, EG7, a T-cell lymphoblastic cell line, NIH3T3, a mouse embryo fibroblast cell line, and RAW264, a mouse leukemic monocyte cell line, were purchased from ATCC. B16-BL6, a mouse melanoma cell line, was purchased from Riken Cell Bank. L5178Y cells were kindly gifted from Dr. Ichii (Osaka University).

Plasmids

The expression vector of Flag-hRhoA G14V was the kind gift of Prof. Kaibuchi (Nagoya University). The expression vector of C-terminal 3×Flag tag-fused AKAP13 was constructed by inserting the human AKAP13 coding sequence into pCI-neo (Promega, WI). The AKAP13 coding sequence was obtained by PCR using pEGFP-Flag-AKAP13 (Addgene, #67571). To construct CD47 expression vector, murine Cd47 cDNA was obtained from murine spleen cDNA by PCR and then inserted to pBABEpuro vector.

To construct the expression vector of EGFRΔcytosol/CD47 cytosol chimera protein, cDNA of cytosol domain-deleted EGFR (1 - 644 AA) was amplified from pCI-neo-EGFR-HA by PCR and inserted into pCI-neo. Oligo DNA of the CD47 cytosol domain (305–324 AA) was then inserted into the pCI-neo-EGFRΔcytosol behind EGFR sequences. p115-GEF cDNA was cloned from cDNA of HeLa cells and then inserted into pFlagCMV2 (SIGMA). PDZ-GEF cDNA was amplified from pCMV-Myc-PDZ GEF and inserted into pFlagCMV2. pCMV-Myc-PDZ GEF was the kind gift from Prof. Inagaki (Osaka University) (7).

Knockdown

For knockdown of CD47 and AKAP13, siRNA was transfected into HeLa cells using Lipofectamine RNAi MAX (Thermo Fisher Scientific, Inc., MA) according to the manufacturer's instruction. siRNAs for CD47 and AKAP13 were purchased from Shanghai Gene Pharma (Shanghai, China). For lentiviral knockdown of CD47 and AKAP13, the oligo DNA was inserted into pLKO.1puro and then CD47- and AKAP13-knockdowned HeLa, EG7 and L5178Y cells were prepared as described previously (8). The siRNA and shRNA sequences are described below: human siCD47 sense, 5'-CCAAAUGAAAAUAUUCUUATT-3'; human siAKAP13 sense, 5'-CGUGAAAGCUGAAGAUGAATT-3'; human shCD47 sense, 5'-AACTACACTTGTGAAGTAACA-3'; mouse shCD47#1 sense, 5'-AGCTCAACTACTGTTTAGTAA-3'; mouse shCD47#2 sense, 5'-AGCAGAACTACTTGGATTAGT-3'; mouse shAkap13 sense, 5'-AACTCTTTGATGTCACTTTCA-3'.

Flowcytometry

Integrins and immune checkpoint molecules in EG7 cells were stained with the following antibodies: anti-α4 antibody (R1-2; GeneTex, Inc., CA), anti-αv antibody (RMV-7; BioLegend, Inc., CA), anti-CD29 antibody (HMβ1; BioLegend), and anti-β3 antibody (2C9.G2; BioLegend); anti-CTLA-4 antibody (UC10-4B9, BioLegend); anti-PD-L1 antibody (10F.9G2, BioLegend); anti-PD-1 antibody (J43, eBioscience). They were then analyzed with a Gallios flowcytometer (Beckman Coulter, Inc., CA).

Preparation of CD47-deficient cells

To construct the CD47-targeted sgRNA-expressing vectors, the oligo DNA from murine CD47 exon 2 (5'-GGATAAGCGCGATGCCATGG-3') was inserted into the BbsI site of pX330-U6-Chimeric_BB-CBh-hSpCas9 (Addgene). DNA fragments of murine CD47 exon 2 were inserted into the BamHI and EcoRI sites of pCAG-EGxxFP, which was the kind gift of Prof. Ikawa (Osaka University) (9). These plasmids were electroporated into EG7 cells with a GenePulser II (Bio-Rad Laboratories, Inc., CA), and EGFP-positive cells were sorted with a SH800 (SONY Co., Tokyo, Japan). After cloning, CD47 deficiency in the cells was confirmed by sequence analysis and FACS using an anti-CD47 antibody

(miap301; Biolegend). CD47 KO EG7 cells were electroporated with pBABEpuro-CD47 with a GenePulser II and then selected with 1 μg/ml puromycin for 48 h. CD47 expression-recovered EG7 cells were sorted with a SH800

Purification of recombinant protein

The DNA sequence of the CD47 cytosol domain (305–324 AA) was inserted into the BamHI and XhoI sites of pGEX6P-1. The DNA sequences of the N-terminal Myc-tagged AKAP13 DHPH domain (1973–2342 AA), DH domain (1976–2211 AA) and PH domain (2212–2342 AA) were obtained by PCR using pEGFP-Flag-AKAP13 and inserted into the BamHI and XhoI sites of pCold II. pGEX4T-1-p21 PBD was kindly provided by Prof. Mizuno (Tohoku University). E-coli Rosetta 2 (DE3) cells carrying these vectors were cultured in LB medium at 37°C until the OD600 reached 0.4, and then the cells were cultured in LB medium containing 0.1 mM IPTG for 24 h at 16°C. After washing the cells with PBS (-), the cells were disrupted with a sonicator (Sonifier 450; BRANSON) and centrifuged at 12,000*g* for 15 min. The supernatant was incubated with glutathione beads (glutathione Sepharose 4B; GE Healthcare, WI) or Ni-NTA agarose beads (WAKO, Osaka, Japan) for 2 h at 4°C and then the protein was eluted in 20 mM glutathione, 100 mM Tris-HCl pH 9.0 or 0.5 M imidazole, 20 mM Tris-HCl pH 8.0, 150 mM NaCl, 0.1% NP-40. Glutathione and imidazole were removed from the protein by size-exclusion centrifugation.

Phagocytosis assay

For preparation of bone marrow-derived macrophages (BMM), bone marrow cells were obtained from the tibias and femurs of C57BL6 mice (female, 8 weeks) and cultured for 6 days in RPMI1640 containing 10% FBS and 10 ng/ml recombinant murine M-CSF (PeproTech, Inc., NJ). Bone marrow-derived GM-CSF-induced dendritic cells (GMDC) were prepared by culturing bone marrow cells for 7 days with 10 ng/ml recombinant murine GM-CSF (PeproTech). EG7 cells were stained using 10 μM CMTMR (Thermo Fisher Scientific) for 30 min at 37°C. After washing, stained EG7 cells were co-cultured for 2 h with BMM or GMDC, and then BMM and GMDC were stained using anti-CD11b-APC and anti-CD11c-APC (BioLegend). Dead EG7 cells were prepared by culturing the cells for 48 h in serum-free RPMI1640. EG7 cell-engulfed BMM and GMDC were analyzed with a Gallios flowcytometer and confocal microscopy (FV-10; Olympus Co., Tokyo, Japan).

Tumor transplantation

EG7 cells (5.0×10^5 cells/200 μl) were subcutaneously injected into the right flank of C57BL6 mice (female, 8 weeks). Tumor volume was calculated by the formula [volume = $0.52 \times (\text{width})^2 \times \text{length}$]. Tumor diameter was measured with a caliper. For the tumor metastasis model, 1.0×10^5 EG7 cells were injected into the tail vein of C57BL6 mice (female, 8 weeks). For the macrophage-depletion model,

clodronate-containing liposomes were intraperitoneally injected to C57BL6 mice, and then EG7 cells were inoculated in the mice by i.v. at 24 h after the liposome injection. L5178Y cells (1.0×10^5 cells/1 ml) were intraperitoneally injected into BALB/c mice (female, 8 weeks).

Microscopy

HeLa cells were grown on 12 mm glass coverslips and transfected with expression vectors of Flag-RhoA G14V and AKAP13-Flag using jetPEI (Polyplus-transfection, Illkirch, France) according to the manufacturer's instructions. The cells were fixed and stained with 0.5 μg/ml Hoechst 33342 and rhodamine-phalloidin (Thermo Fisher Scientific) at 48 h post-transfection. The samples were then observed using a FV-10 confocal microscope.

Pulldown of activated RhoA and Rac1

EG7 cells were stimulated with 200 ng/ml recombinant murine TSP-1 (R&D Systems, Inc., MN) for the indicated period and lysed in 20 mM Tris-HCl pH 8.0, 150 mM NaCl, 0.5% NP-40, 5 mM $MgCl_2$, 1 mM DTT, and 5 mM NaF. The lysate was incubated with 10 μg of GST-PBD together with glutathione beads for 2 h at 4°C. Precipitated samples were immunoblotted using anti-RhoA antibody (× 200, 67B9; Cell Signaling Technology, MA), anti-Rac1 antibody (× 1000; BD) and anti-GST antibody (× 1000; Santacruz Biotechnology, Inc., TX).

Immunoprecipitation

HEK293T cells were transfected with pCIneo-AKAP13-Flag using PEI Max (MW: 40000; Polyscience, Inc., PA) and then lysed in 20 mM Tris-HCl pH 8.0, 150 mM NaCl, 1% NP-40, and 5 mM EDTA at 48 h post-transfection by sonication. The lysate was immunoprecipitated for 2 h using anti-FLAG antibody (M2; Sigma-Aldrich) at 4°C, and then the beads were washed three times and incubated with 30 μg of recombinant GST or GST-CD47-cytosol domain in 20 mM Tris-HCl pH 8.0, 150 mM NaCl, 0.5% NP-40, and 5 mM $MgCl_2$ for 2 h at 4°C. After washing, the samples were boiled in 2× SDS sample buffer for 5 min and immunoblotted.

WST assay

EG7 cells (7.5×10^3 cells/100 μl) were seeded in a 96-well plate and supplemented with 10 μl of Cell Counting Kit-8 solution (DOJINDO Laboratories, Inc., Kumamoto, Japan). After incubation for 1.5 h, the OD450 was measured with a plate reader (iMark; Bio-Rad Laboratories).

Cell migration assay

The method used to quantify cell migration was described previously (10). Briefly, 5.0×10^5 EG7 cells were added to the upper chamber of a 24-well Transwell plate (8 μm pore size), and the lower chamber was filled with RPMI1640 containing 1% FBS and 1 μg/ml recombinant murine SDF-1α (BioLegend). After 16 h incubation at 37°C, the cells in the lower chamber were transferred to a 96-well plate and Cell Counting Kit-8 solution was added. The cells were cultured for 16 h at 37°C, and then OD450 was measured as described above.

Results

Generation of CD47-deficient EG7 cells

First, Cd47 mRNA expression was quantified in various murine tissues and cell lines by qPCR (Fig. 1A). Since Cd47 mRNA expression was high in EG7 cells, we investigated the contribution of CD47 to lymphoma metastasis and tumor formation by generating CD47-deficient EG7 cells with a Cas-CRISPR system (Fig. 1B). CD47 knockout (KO) EG7 cells carried a frameshift mutation in the CD47 exon 2 locus and abolished CD47 expression on the cell surface (Fig. 1C and D).

CD47 is required for lymphoma tumor formation and metastasis

We then asked whether CD47 contributes to tumor formation and metastasis *in vivo*. Our results showed that CD47 deficiency decreases tumor growth and the tumor formation rate in a subcutaneous transplantation model (Fig. 2A and B). In the tumor metastasis model, wild-type EG7 cells were metastasized to the liver and intraperitoneal cavity, leading to death of the mice within 40 days after intravenous injection, but CD47 KO EG7 cells did not establish liver metastasis, and all the mice injected with these cells were still alive more than 50 days after injection (Fig. 2C, D and E). Ectopic CD47 expression in CD47 KO EG7 cells worsened the survival of the EG7 cells-injected mice (Fig. 2F and G). To investigate whether CD47 promotes T-cell lymphoma metastasis and, if so, whether such promotion is dependent on the anti-phagocytic function of CD47, we prepared macrophage-depleted mice by injecting clodronate-containing liposomes (Fig. 2H). Intravenously injected CD47 KO EG7 cells did not form tumors in macrophage-depleted mice (Fig. 2I). Moreover, we investigated CD47 contribution to the tumor formation of L5178Y cells, thymic tumor-derived lymphoma cell line. CD47 shRNA-expressing L5178Y cells had less capability for tumor formation than control shRNA-expressing L5178Y cells (Fig. 2J). Expression of immune checkpoint molecules was comparable between wild-type and CD47 KO EG7 cells (Fig. 2K). These data indicated that CD47 is essential for T-cell lymphoma metastasis *in vivo* independent of its anti-phagocytic function.

CD47 deficiency in EG7 cells did not affect the phagocytic efficiency of macrophages and dendritic cells

We then investigated whether CD47 deficiency affects cell proliferation and migration *in vitro*. Our results showed that cell proliferation and SDF-1α-induced migration were not significantly different between wild-type and CD47 KO EG7 cells (Fig. 3A and B). Since previous studies showed that CD47 contributes to α4β1 and αvβ3 integrin-mediated cell attachment, we investigated the relation between expression of these integrins and integrin-mediated cell attachment (11). We found that α4β1 expression was elevated in CD47-deficient cells, but αvβ3 integrin was not detected in EG7 cells (Fig. 3C). CD47-deficiency did not alter the attachment of EG7 cells to fibronectin, which has a binding motif of various integrin family proteins, including α4β1 and αvβ3 (Fig. 3D). Thus, integrin-mediated cell attachment was comparable between wild-type and CD47 KO EG7 cells, and CD47 did not contribute to cell proliferation and migration *in vitro*.

Next, we investigated whether CD47-deficency promotes phagocytosis of EG7 by macrophages and dendritic cells in vitro. For this purpose, live and dead EG7 cells were co-cultured with BMM or GMDC, and then $CMTMR^+$ $CD11b^+$ cells (EG7 cell-engulfed BMM) and $CMTMR^+$ $CD11c^+$ cells (EG7 cell-engulfed GMDC) were quantified by FACS. The phagocytotic efficiency of CD47 KO cells by BMM and GM-DC was compatible with that of wild-type EG7 cells, irrespective of whether the cells were dead or alive (Fig. 3E, F, G and H). Similarly, CD47 knockdown in L5178Y cells was not affected phagocytic efficiency of L5178Y cells by macrophages (Fig. 3I and J). Microscopy of the EG7 cell-engulfed BMM showed the same results as described above (Fig. 3K). These data indicate that CD47 does not contribute to the phagocytic efficiency of EG7 lymphoma cells by macrophages and dendritic cells *in vitro*.

CD47 is required for the basal activity of RhoA in EG7 cells

Previous studies showed that TSP-1, the ligand for CD47, alters RhoA and Rac1 activities via CD47, and RhoA and Rac1 levels are closely correlated with lymphoma metastasis (3). Thus, we speculated that CD47 deficiency decreases RhoA and Rac1 activities in EG7 cells, resulting in the low efficiency of tumor formation and metastasis. Our experiments showed that activated RhoA was significantly decreased in CD47 KO EG7 cells (Fig. 4A and B), but the Rac1 activities were comparable between wild-type and CD47 KO EG7 cells (Fig. 4C and D). After TSP-1 stimulation, RhoA and Rac1 activities were upregulated in wild-type EG7 cells but not CD47 KO cells (Fig. 4E and F). To determine whether the low metastatic activity of CD47 KO EG7 cells is due to RhoA downregulation, we prepared RhoA G14V-expressing EG7 cells, which is constitutive active mutant of RhoA (Fig. 4G). The tumor formation of CD47 KO EG7 cells was recovered by RhoA G14V expression in a tumor metastatic model (Fig. 4H). These results showed that CD47 deficiency decrease RhoA activity with or without TSP-1 stimulation, resulting in the low efficiency of T-cell lymphoma metastasis.

CD47 upregulates AKAP13-mediated RhoA activation

Since our data showed that CD47 upregulates basal RhoA activity but not basal Rac1 activity, we speculated that CD47 regulates RhoA via RhoA-specific GEFs or GAPs, such as AKAP13, PDZ-GEF and p115-RhoGEF. Among them, we focused on the correlation between CD47 and AKAP13, one of the RhoA-specific GEFs, because previous studies showed that CD47-deficient mice expressed similar phenotypes as AKAP13 mutant mice in terms of bone formation and immune responses (12-15). Basal RhoA activities were decreased by siRNA-mediated CD47 and AKAP13 knockdown in HeLa cells (Fig. 5A). AKAP13 directly interacts with the cytosolic domain of CD47 via its PH domain (Fig. 5B and C). Previous studies showed that RhoA interacts with the AKAP13 DH domain, though this interaction was decreased in CD47 KO EG7 cells (Fig. 5D) (16). RhoA did not interact with the CD47 cytosolic domain directly, but rather bound this domain indirectly via the AKAP13 DHPH domain, indicating that these molecules form a RhoA-AKAP13-CD47 complex (Fig. 5E). CD47 cytosolic domain interacts with AKAP13 but not other RhoA-specific GEFs, PDZ-GEF and p115-GEF (Fig. 5F). To investigate whether CD47 cytosolic domain upregulates RhoA activity dependent on its ligand, we prepared an expression vector of chimera protein of EGFR Δcytosolic domain-CD47 cytosolic domain This chimera protein increased RhoA activity in CD47-deficient EG7 cells, indicating that CD47 cytosolic domain upregulates RhoA activity independent on TSP-1 stimulation (Fig. 5G). AKAP13-mediated RhoA upregulation and stress fiber formation were canceled by CD47 downregulation, but RhoA G14V-induced stress fiber formation was not affected by CD47 knockdown (Fig. 5H, I and J). Moreover, AKAP13 knockdown did not affect the expression of CD47 but decreased EG7 tumor formation efficiency (Fig. 5K, L and M). These data indicated that CD47 forms a complex with RhoA and AKAP13 and acts as a scaffold for AKAP13-mediated RhoA activation, which is required for T-cell lymphoma progression.

Discussion

CD47 levels are known to correlate with various cellular functions and signaling pathways, such as integrin-mediated cell adhesion, TSP-1-induced RhoA and Rac1 activation and phagocytosis (2). Since RhoA and Rac1 activity contribute to lymphoma metastasis, we considered that CD47 might be correlated with the prognosis of lymphoma. In this study, we demonstrated that CD47 upregulates basal RhoA activity by facilitating RhoA-AKAP13 complex formation without TSP-1 stimulation, which promotes T-cell lymphoma tumor formation and metastasis. Although there are several RhoA-related GEFs, such as LARG, p115 RhoA-GEF and PDZ-GEF, as well as AKAP13, CD47 selectively interacts with AKAP13 (Fig. 5F), suggesting that CD47-AKAP13 interaction may provide a unique scaffold for AKAP13-mediated RhoA activation. AKAP13 interacts with RhoA via its DH domain, which is highly conserved among RhoA GEFs. AKAP13 interacts with CD47 via its PH domain, which shows low homology with other GEFs, leading to AKAP13-specific CD47 interaction and regulation (17). In agreement with this, our data demonstrated that the CD47 cytosolic domain interacts with the PH domain of AKAP13 and facilitates AKAP13-RhoA complex formation and that AKAP13-mediated RhoA activation was not induced in CD47 KO cells (Fig. 5E and H).

Lymphocytes express various integrin family proteins that promote cell attachment and homing and also correlate with lymphoma metastasis (18,19). αvβ3 integrin promotes proliferation and liver metastasis of lymphoma, and a neutralizing antibody against α4β1 integrin represses lymphoma proliferation by inhibiting lymphoma-stromal cell interaction (20,21). Our data showed that EG7 cells, a T-cell lymphoblastic cell line, did not express αvβ3 integrin, and integrin-mediated cell attachment was not affected by CD47 deficiency despite increased expression of α4 and β1 integrin in CD47 KO cells (Fig. 3C and D). These results suggest that α4β1 integrin weakly contributes to cell attachment of EG7 cells and the contribution of CD47 to integrin-mediated cell attachment is dependent on the cell type. In support of this idea, a previous study showed that CD47 is not required for α4β1 and α5β1 integrin-mediated cell adhesion in T cells (22).

Previous studies showed that CD47 inhibition facilitates cancer engulfment by phagocytes, and development of a CD47 neutralizing antibody for cancer treatment is currently proceeding to clinical trials. Moreover, CD47 inhibition has been shown to activate STING-mediated innate immune signaling and tumor antigen-induced tumor immunity in a tumor-bearing mouse model (23,24). Our data showed that the phagocytic efficiency of CD47-deficient EG7 cells by phagocytes was similar to that of wild-type EG7 cells, but CD47 KO EG7 cells did not form tumors by intravenous injection (Fig. 2C and Fig. 3E-3K). Another group showed that a CD47 neutralizing antibody induces phagocytosis in B cell- and myeloid-derived cancer cells but not in a T-cell-derived cell line (25). These results suggest that other unknown anti-phagocytic molecules contribute to the "Don't eat me signaling" in T-cell lymphoma cells, including EG7 cells (26). Thus, in our experimental model, CD47-mediated RhoA activation made a greater contribution to T-cell lymphoma metastasis and tumor formation than the anti-phagocytic function of CD47 did.

RhoA is one of the attractive targets for cancer treatment due to its importance for cancer proliferation and metastasis. Recent studies showed that Y16 inhibits LARG-RhoA interaction, leading to the suppression of MCF7 tumor sphere formation (4). Similarly, inhibition of the CD47-AKAP13 interaction has the potential to repress T-cell lymphoma metastasis. Our data showed that the cytosolic domain of CD47 interacts with the PH domain of AKAP13, suggesting that an AKAP13 PH domain-derived peptide inhibits CD47-AKAP13 interaction and T-cell lymphoma metastasis by conjugating a cell penetrating sequence, such as TAT and octaarginine. Moreover, chemicals which inhibit CD47-AKAP13 interaction also have potential for use in a new treatment of T-cell lymphoma. Taken together, our results show that CD47 promotes T-cell lymphoma metastasis by upregulating AKAP13-meditaed RhoA activation independent of its anti-phagocytic function, and that the CD47-AKAP13 interaction would be a novel target for T-cell lymphoma treatment.

Author contributions

Y.K, M.I, K.S, N.M, K.Owashi and S.Y performed experiments. R.M, J.K and K.Oritani analyzed the data. Y.K wrote the paper. Y.K and T.M designed and supervised the project.

Funding

This study was supported in part by Grant-in-Aid for Scientific Research (B) 19H03364 (T.M) and Grant-in-Aid for Early-Career Scientists 18K14893 (Y.K). This work was the result of using research equipment shared in MEXT Project for promoting public utilization of advanced research infrastructure (Program for supporting introduction of the new sharing system) Grant Number JPMXS0420100119. This research was partially supported by Platform Project for Supporting Drug Discovery and Life Science Research (Basis for Supporting Innovative Drug Discovery and Life Science Research (BINDS)) from AMED under Grant Number JP19am0101093 (support number 1234).

Conflict of Interest: All authors declare no conflicts of interest in regards to this manuscript

Reference

1. Erter, J., Alinari, L., Darabi, K., Gurcan, M., Garzon, R., Marcucci, G., Bechtel, M. A., Wong, H., and Porcu, P. (2010) New targets of therapy in T-cell lymphomas. *Curr Drug Targets* **11**, 482-493
2. Brown, E. J., and Frazier, W. A. (2001) Integrin-associated protein (CD47) and its ligands. *Trends Cell Biol* **11**, 130-135
3. Svensmark, J. H., and Brakebusch, C. (2019) Rho GTPases in cancer: friend or foe? *Oncogene* **38**, 7447-7456
4. Shang, X., Marchioni, F., Evelyn, C. R., Sipes, N., Zhou, X., Seibel, W., Wortman, M., and Zheng, Y. (2013) Small-molecule inhibitors targeting G-protein-coupled Rho guanine nucleotide exchange factors. *Proc Natl Acad Sci U S A* **110**, 3155-3160
5. Feng, M., Jiang, W., Kim, B. Y. S., Zhang, C. C., Fu, Y. X., and Weissman, I. L. (2019) Phagocytosis checkpoints as new targets for cancer immunotherapy. *Nat Rev Cancer* **19**, 568-586
6. Advani, R., Flinn, I., Popplewell, L., Forero, A., Bartlett, N. L., Ghosh, N., Kline, J., Roschewski, M., LaCasce, A., Collins, G. P., Tran, T., Lynn, J., Chen, J. Y., Volkmer, J. P., Agoram, B., Huang, J., Majeti, R., Weissman, I. L., Takimoto, C. H., Chao, M. P., and Smith, S. M. (2018) CD47 Blockade by Hu5F9-G4 and Rituximab in Non-Hodgkins Lymphoma. *N Engl J Med* **379**, 1711-1721
7. Hirotani, M., Ohoka, Y., Yamamoto, T., Nirasawa, H., Furuyama, T., Kogo, M., Matsuya, T., and Inagaki, S. (2002) Interaction of plexin-B1 with PDZ domain-containing Rho guanine nucleotide exchange factors. *Biochem Biophys Res Commun* **297**, 32-37
8. Kitai, Y., Iwakami, M., Saitoh, K., Togi, S., Isayama, S., Sekine, Y., Muromoto, R., Kashiwakura, J., Yoshimura, A., Oritani, K., and Matsuda, T. (2017) STAP-2 protein promotes prostate cancer growth by enhancing epidermal growth factor receptor stabilization. *J Biol Chem* **292**, 19392-19399

9. Mashiko, D., Fujihara, Y., Satouh, Y., Miyata, H., Isotani, A., and Ikawa, M. (2013) Generation of mutant mice by pronuclear injection of circular plasmid expressing Cas9 and single guided RNA. *Sci Rep* **3**, 3355
10. Matsumoto, N., Kon, S., Nakatsuru, T., Miyashita, T., Inui, K., Saitoh, K., Kitai, Y., Muromoto, R., Kashiwakura, J. I., Uede, T., and Matsuda, T. (2017) A Novel alpha9 Integrin Ligand, XCL1/Lymphotactin, Is Involved in the Development of Murine Models of Autoimmune Diseases. *J Immunol* **199**, 82-90
11. Barazi, H. O., Li, Z., Cashel, J. A., Krutzsch, H. C., Annis, D. S., Mosher, D. F., and Roberts, D. D. (2002) Regulation of integrin function by CD47 ligands. Differential effects on alpha vbeta 3 and alpha 4beta1 integrin-mediated adhesion. *J Biol Chem* **277**, 42859-42866
12. Chin, A. C., Fournier, B., Peatman, E. J., Reaves, T. A., Lee, W. Y., and Parkos, C. A. (2009) CD47 and TLR-2 cross-talk regulates neutrophil transmigration. *J Immunol* **183**, 5957-5963
13. Shibolet, O., Giallourakis, C., Rosenberg, I., Mueller, T., Xavier, R. J., and Podolsky, D. K. (2007) AKAP13, a RhoA GTPase-specific guanine exchange factor, is a novel regulator of TLR2 signaling. *J Biol Chem* **282**, 35308-35317
14. Koide, H., Holmbeck, K., Lui, J. C., Guo, X. C., Driggers, P., Chu, T., Tatsuno, I., Quaglieri, C., Kino, T., Baron, J., Young, M. F., Robey, P. G., and Segars, J. H. (2015) Mice Deficient in AKAP13 (BRX) Are Osteoporotic and Have Impaired Osteogenesis. *J Bone Miner Res* **30**, 1887-1895
15. Uluckan, O., Becker, S. N., Deng, H., Zou, W., Prior, J. L., Piwnica-Worms, D., Frazier, W. A., and Weilbaecher, K. N. (2009) CD47 regulates bone mass and tumor metastasis to bone. *Cancer Res* **69**, 3196-3204
16. Schrade, K., Troger, J., Eldahshan, A., Zuhlke, K., Abdul Azeez, K. R., Elkins, J. M., Neuenschwander, M., Oder, A., Elkewedi, M., Jaksch, S., Andrae, K., Li, J., Fernandes, J., Muller, P. M., Grunwald, S., Marino, S. F., Vukicevic, T., Eichhorst, J., Wiesner, B., Weber, M., Kapiloff, M., Rocks, O., Daumke, O., Wieland, T., Knapp, S., von Kries, J. P., and Klussmann, E. (2018) An AKAP-Lbc-RhoA interaction inhibitor promotes the translocation of aquaporin-2 to the plasma membrane of renal collecting duct principal cells. *PLoS One* **13**, e0191423
17. Abdul Azeez, K. R., Knapp, S., Fernandes, J. M., Klussmann, E., and Elkins, J. M. (2014) The crystal structure of the RhoA-AKAP-Lbc DH-PH domain complex. *Biochem J* **464**, 231-239
18. Dustin, M. L. (2019) Integrins and Their Role in Immune Cell Adhesion. *Cell* **177**, 499-501
19. Mraz, M., Zent, C. S., Church, A. K., Jelinek, D. F., Wu, X., Pospisilova, S., Ansell, S. M., Novak, A. J., Kay, N. E., Witzig, T. E., and Nowakowski, G. S. (2011) Bone marrow stromal cells protect lymphoma B-cells from rituximab-induced apoptosis and targeting integrin alpha-4-beta-1 (VLA-4) with natalizumab can overcome this resistance. *Br J Haematol* **155**, 53-64
20. Yun, Z., Smith, T. W., Menter, D. G., McIntire, L. V., and Nicolson, G. L. (1997) Differential adhesion of metastatic RAW117 large-cell lymphoma cells under static or hydrodynamic conditions: role of integrin alpha(v) beta3. *Clin Exp Metastasis* **15**, 3-11

21. Cayrol, F., Diaz Flaque, M. C., Fernando, T., Yang, S. N., Sterle, H. A., Bolontrade, M., Amoros, M., Isse, B., Farias, R. N., Ahn, H., Tian, Y. F., Tabbo, F., Singh, A., Inghirami, G., Cerchietti, L., and Cremaschi, G. A. (2015) Integrin alphavbeta3 acting as membrane receptor for thyroid hormones mediates angiogenesis in malignant T cells. *Blood* **125**, 841-851
22. Li, Z., Calzada, M. J., Sipes, J. M., Cashel, J. A., Krutzsch, H. C., Annis, D. S., Mosher, D. F., and Roberts, D. D. (2002) Interactions of thrombospondins with alpha4beta1 integrin and CD47 differentially modulate T cell behavior. *J Cell Biol* **157**, 509-519
23. Liu, X., Pu, Y., Cron, K., Deng, L., Kline, J., Frazier, W. A., Xu, H., Peng, H., Fu, Y. X., and Xu, M. M. (2015) CD47 blockade triggers T cell-mediated destruction of immunogenic tumors. *Nat Med* **21**, 1209-1215
24. von Roemeling, C. A., Wang, Y., Qie, Y., Yuan, H., Zhao, H., Liu, X., Yang, Z., Yang, M., Deng, W., Bruno, K. A., Chan, C. K., Lee, A. S., Rosenfeld, S. S., Yun, K., Johnson, A. J., Mitchell, D. A., Jiang, W., and Kim, B. Y. S. (2020) Therapeutic modulation of phagocytosis in glioblastoma can activate both innate and adaptive antitumour immunity. *Nat Commun* **11**, 1508
25. Chen, J., Zhong, M. C., Guo, H., Davidson, D., Mishel, S., Lu, Y., Rhee, I., Perez-Quintero, L. A., Zhang, S., Cruz-Munoz, M. E., Wu, N., Vinh, D. C., Sinha, M., Calderon, V., Lowell, C. A., Danska, J. S., and Veillette, A. (2017) SLAMF7 is critical for phagocytosis of haematopoietic tumour cells via Mac-1 integrin. *Nature* **544**, 493-497
26. Barkal, A. A., Brewer, R. E., Markovic, M., Kowarsky, M., Barkal, S. A., Zaro, B. W., Krishnan, V., Hatakeyama, J., Dorigo, O., Barkal, L. J., and Weissman, I. L. (2019) CD24 signalling through macrophage Siglec-10 is a target for cancer immunotherapy. *Nature* **572**, 392-396

Abbreviations

BMM: bone marrow-derived macrophages
GAP: GTPase-activating protein
GEF: guanine nucleotide exchange factor
GMDC: bone marrow-derived GM-CSF-induced dendritic cells

Figure legends

Figure 1. Generation of CD47-deficient EG7 cells
A. Expression of Cd47 mRNA in various murine tissues and cell lines was measured by qPCR. (n = 3). The mean values and standard errors are depicted. **B.** Schematic representation of CD47-targeted sgRNA sequences. **C.** Genomic sequences from CD47-deficient EG7 cells. **D.** FACS analysis of CD47 expression in EG7 cells.

Figure 2. CD47-deficiency decreases tumor formation

A. EG7 cells were subcutaneously injected into the right flank of C57BL/6 mice and the tumor volume was measured. **B.** The rate of EG7 tumor establishment by s.c. injection. **C, D.** EG7 cells were intravenously injected into the tail vein of C57BL/6 mice. The survival rates of the mice and representative images are shown. Arrows indicate EG7 tumors in peritoneal cavity. **E.** EG7 cells were injected in the same manner as in **C**, and then the paraffin-embedded mouse liver was stained by hematoxylin and eosin at Day 30. **F.** CD47 KO EG7 cells were electroporated with CD47 expression vector and then recovery of CD47 expression was confirmed by FACS. **G.** CD47 expression-recovered EG7 cells were intravenously injected to C57BL/6 mice and the survival rates of the mice are shown. **H, I.** Macrophages in the C57BL/6 mice were depleted by intraperitoneal injection of clodronate-containing liposomes, followed by intravenous injection of EG7 cells. Macrophages depletion in splenocytes was validated by FACS. The survival rates of the mice are shown (n = 5). **J.** CD47 expression in L5178Y cells was knockdowned and confirmed by FACS. **K.** CD47-knockdowned L5178Y cells were intraperitoneally injected to BALB/c mice and the survival rates of the mice are shown (n = 5). **L.** The expression of immune checkpoint molecules in CD47 KO EG7 cells was confirmed by FACS. The mean values and standard errors are depicted. *P < 0.05 (paired Student's *t*-test).

Figure 3. Engulfment of EG7 cells by macrophages is independent on CD47

A. Wild-type and CD47 deficient EG7 cells were cultured for the indicated periods, and then the cell proliferation was evaluated by WST assay. **B.** EG7 cells were cultured in 1 μg/ml SDF-1α with a Transwell plate, and then the migrated cells were quantified by WST assay. **C.** Expression of α4, αv, β1 and β3 integrin in the wild-type and CD47 KO EG7 cells was detected by FACS. The red line represents the results for the negative control, and the blue line represent the results for stained samples. **D.** EG7 cells were cultured in fibronectin-coated dishes, and then the attached cells were quantified by crystal violet staining. **E, F.** CMTMR-stained EG7 cells were co-cultured with bone marrow-derived macrophages (BMM) for 2 h, and then the $CMTMR^+$ cells among $CD11b^+$-gated cells were quantified by FACS. **G, H.** EG7 cells were co-cultured with bone marrow-derived GM-CSF-induced dendritic cells (GMDC) in the same manner as described above, and then the $CMTMR^+$ cells among $CD11c^+$-gated cells were quantified by FACS. **I, J.** CMTMR-stained L5178Y cells were co-cultured with BALB/c-derived BMM and then the BMM were analyzed same as **E**. **K.** CFSE-stained BMM (green) were cocultured with CMTMR-stained EG7 cells (red) for 30 min, and fluorescence was detected by confocal microscopy (n = 3); mean values and standard errors are depicted. N.S = not significant (paired Student's *t*-test).

Figure 4. CD47 is required for basal RhoA activity

A. RhoA-GTP in wild-type and CD47 KO EG7 cells was pulled-down using GST-PBD and glutathione beads, and then immunoblotted. **B.** Band intensity of the pulled-down RhoA/total RhoA was calculated using ImageJ software (n = 4). **C.** Rac1-GTP in wild-type and CD47 KO EG7 cells was pulled-down and (**D)** their band intensities were calculated as described above (n = 6). **E, F.** Wild-type

and CD47 KO EG7 cells were stimulated with 200 ng/ml TSP-1 for the indicated times, and then activated RhoA and Rac1 were pulled-down and blotted. **G, H.** RhoA G14V-stably-expressing EG7 cells were intravenously injected into the tail vein of C57BL/6 mice, and then the survival of the mice was evaluated (n = 5); the mean values and standard errors are depicted. *P < 0.05, **P < 0.01 (paired Student's *t*-test).

Figure 5. CD47 is required for AKAP13-mediated RhoA activation and associates with the AKAP13-RhoA complex.
A. HeLa cells were transiently transfected with CD47 and AKAP13 siRNA, and then activated RhoA in the lysates was pulled-down using GST-PBD and glutathione beads and blotted at 64 h post-transfection. **B.** HEK293T cells were transiently transfected with an expression vector of AKAP13-Flag. The lysates were incubated with recombinant GST or GST-CD47 cytosol and then immunoprecipitated. **C.** Recombinant DHPH, DH and PH domain of AKAP13 were incubated with recombinant GST-CD47 cytosol and then pulled-down using Ni-NTA agarose beads and blotted. **D.** AKAP13-Flag was stably expressed in wild-type and CD47 KO EG7 cells, and then the AKAP13-RhoA complex was immunoprecipitated and blotted. **E.** The lysates of EG7 cells were incubated with recombinant GST-CD47 cytosol and recombinant AKAP13 DHPH for 1 h at 4°C. The AKAP13 DHPH and GST-CD47 cytosol complex was pulled-down using Ni-NTA beads following glutathione beads and then blotted. **F.** HEK293T cells were transiently transfected with an expression vector of AKAP13-Flag, Flag-PDZ and Flag-p115. The lysates were incubated with recombinant GST-CD47 cytosol and then immunoprecipitated. **G.** CD47 KO EG7 cells were transiently transfected with EGFRΔcytosol and EGFRΔcytosol/CD47-cytosol by electroporation and then activated RhoA in the lysates was pulled-down and blotted same as **A** at 48 h post-transfection.
H. Wild-type and CD47 KO EG7 cells were stably expressed AKAP13-Flag, and activated RhoA in the lysates was pulled-down and blotted. **I, J.** shCtrl- and shCD47-expressing HeLa cells were transiently transfected with the expression vectors of Flag-RhoA G14V and AKAP13-Flag and then fixed and stained with Rhodamine-Phalloidin (red) and Hoechst 33342 (blue) at 48 h post-transfection. The images were obtained by confocal microscopy and population of stress fiber-positive cells per 50 cells was counted from the image. **K.** Akap13 mRNA levels in AKAP13-knockdowned EG7 cells were quantified by qPCR. **L.** CD47 expression in AKAP13-knockdowned EG7 cells were measured by FACS. **M.** AKAP13-knockdowned EG7 cells were intravenously injected into the tail vein of C57BL/6 mice. The survival rates of the mice are shown (n = 5). n = 3; mean values and standard errors are depicted. *P < 0.05 (paired Student's *t*-test).

Figure 1

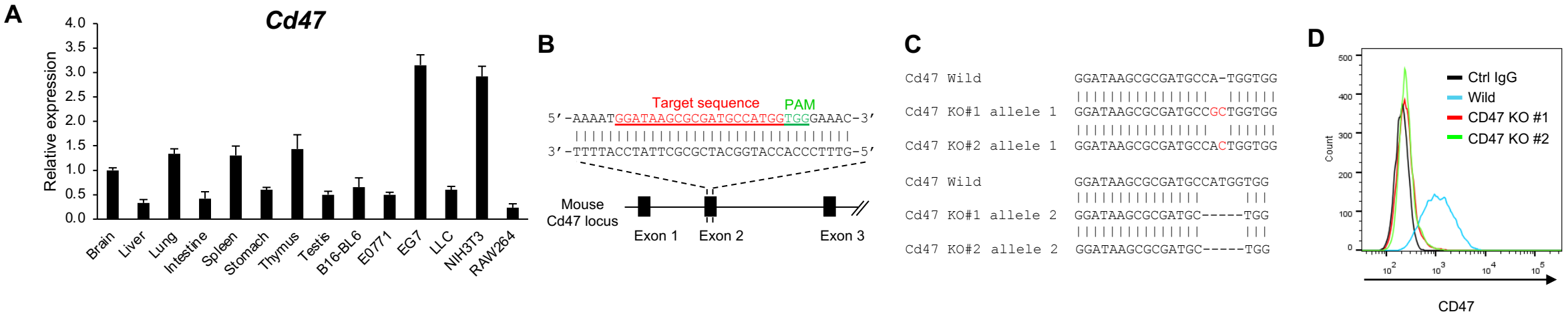
A
Cd47
Relative expression
4.0
3.5
3.0
2.5
2.0
1.5
1.0
0.5
0.0
Brain
Liver
Lung
Intestine
Spleen
Stomach
Thymus
Testis
B16-BL6
E0771
EG7
LLC
NIH3T3
RAW264
B
Target sequence
PAM
5′-AAAATGGATAAGCGCGATGCCATGGTGGGAAAC-3′
3′-TTTTACCTATTCGCGCTACGGTACCACCCTTTG-5′
Mouse
Cd47 locus
Exon 1
Exon 2
Exon 3
C
Cd47 Wild GGATAAGCGCGATGCCA-TGGTGG
Cd47 KO#1 allele 1 GGATAAGCGCGATGCCGCTGGTGG
Cd47 KO#2 allele 1 GGATAAGCGCGATGCCACTGGTGG
Cd47 Wild GGATAAGCGCGATGCCATGGTGG
Cd47 KO#1 allele 2 GGATAAGCGCGATGC-----TGG
Cd47 KO#2 allele 2 GGATAAGCGCGATGC-----TGG
D
Ctrl IgG
Wild
CD47 KO #1
CD47 KO #2
Count
500
400
300
200
100
0
CD47

Figure 2

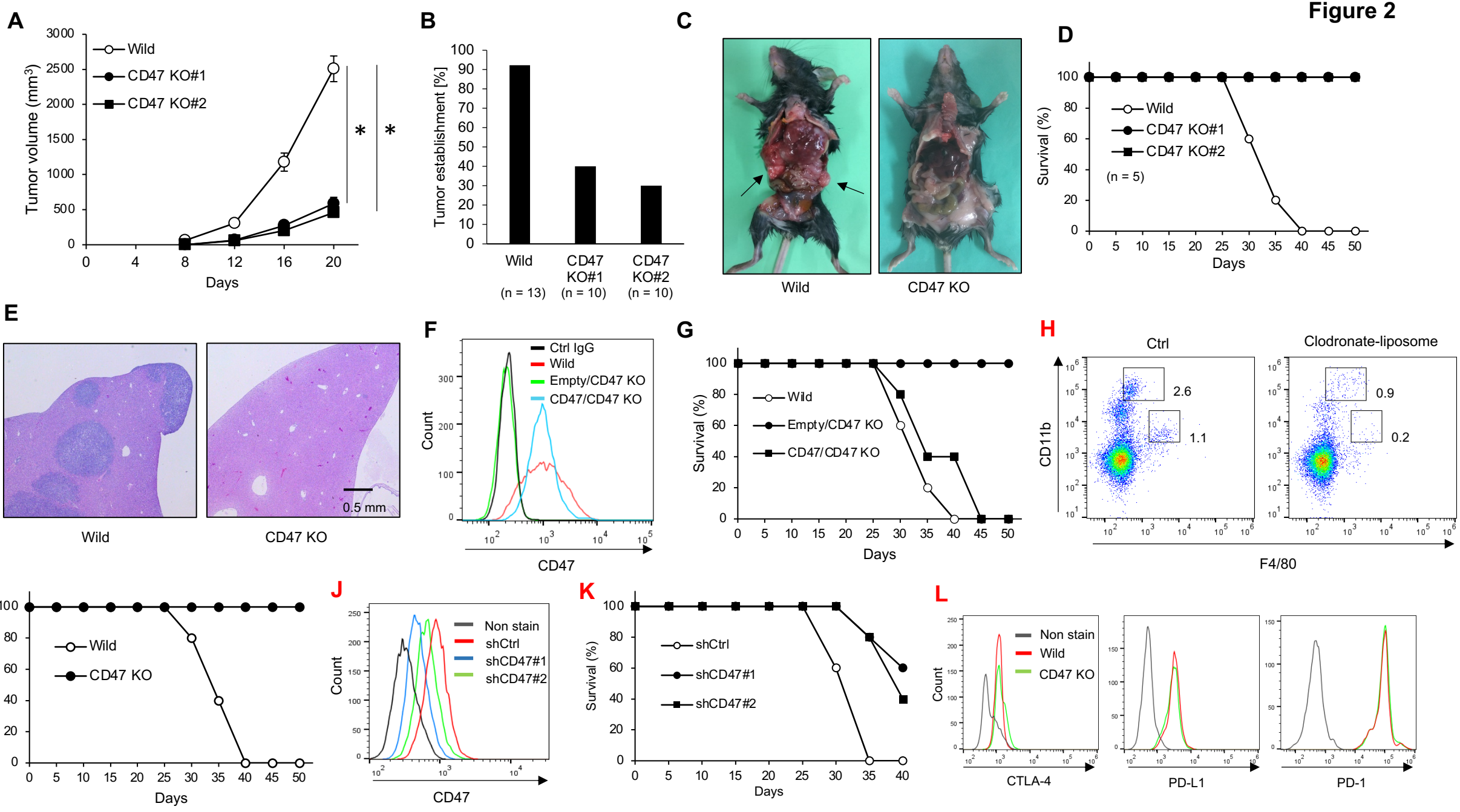
A
Tumor volume (mm3)
Wild
CD47 KO#1
CD47 KO#2
Days
B
Tumor establishment [%]
Wild (n = 13)
CD47 KO#1 (n = 10)
CD47 KO#2 (n = 10)
C
Wild
CD47 KO
D
Survival (%)
Wild
CD47 KO#1
CD47 KO#2
(n = 5)
Days
E
0.5 mm
Wild
CD47 KO
F
Count
Ctrl IgG
Wild
Empty/CD47 KO
CD47/CD47 KO
CD47
G
Survival (%)
Wild
Empty/CD47 KO
CD47/CD47 KO
Days
H
Ctrl
Clodronate-liposome
CD11b
2.6
1.1
0.9
0.2
F4/80
I
Survival (%)
Wild
CD47 KO
Days
J
Count
Non stain
shCtrl
shCD47#1
shCD47#2
CD47
K
Survival (%)
shCtrl
shCD47#1
shCD47#2
Days
L
Count
Non stain
Wild
CD47 KO
CTLA-4
PD-L1
PD-1

Figure 3

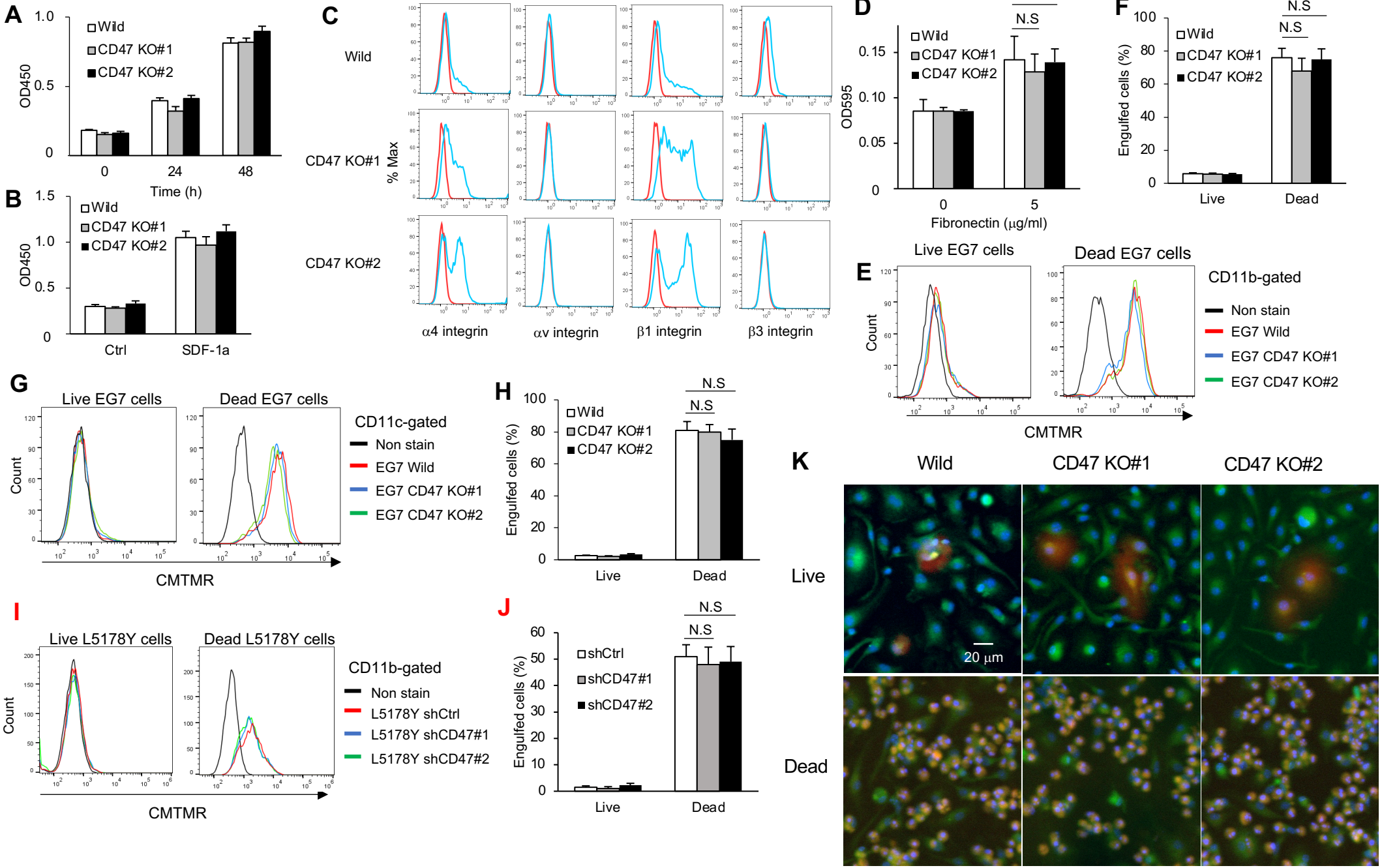
A
OD450
Wild
CD47 KO#1
CD47 KO#2
Time (h)
B
Ctrl
SDF-1a
C
Wild
CD47 KO#1
CD47 KO#2
% Max
α4 integrin
αv integrin
β1 integrin
β3 integrin
D
OD595
Fibronectin (μg/ml)
N.S
E
Live EG7 cells
Dead EG7 cells
Count
CMTMR
CD11b-gated
Non stain
EG7 Wild
EG7 CD47 KO#1
EG7 CD47 KO#2
F
Engulfed cells (%)
Live
Dead
G
CD11c-gated
H
I
Live L5178Y cells
Dead L5178Y cells
L5178Y shCtrl
L5178Y shCD47#1
L5178Y shCD47#2
J
shCtrl
shCD47#1
shCD47#2
K
20 μm

Figure 4

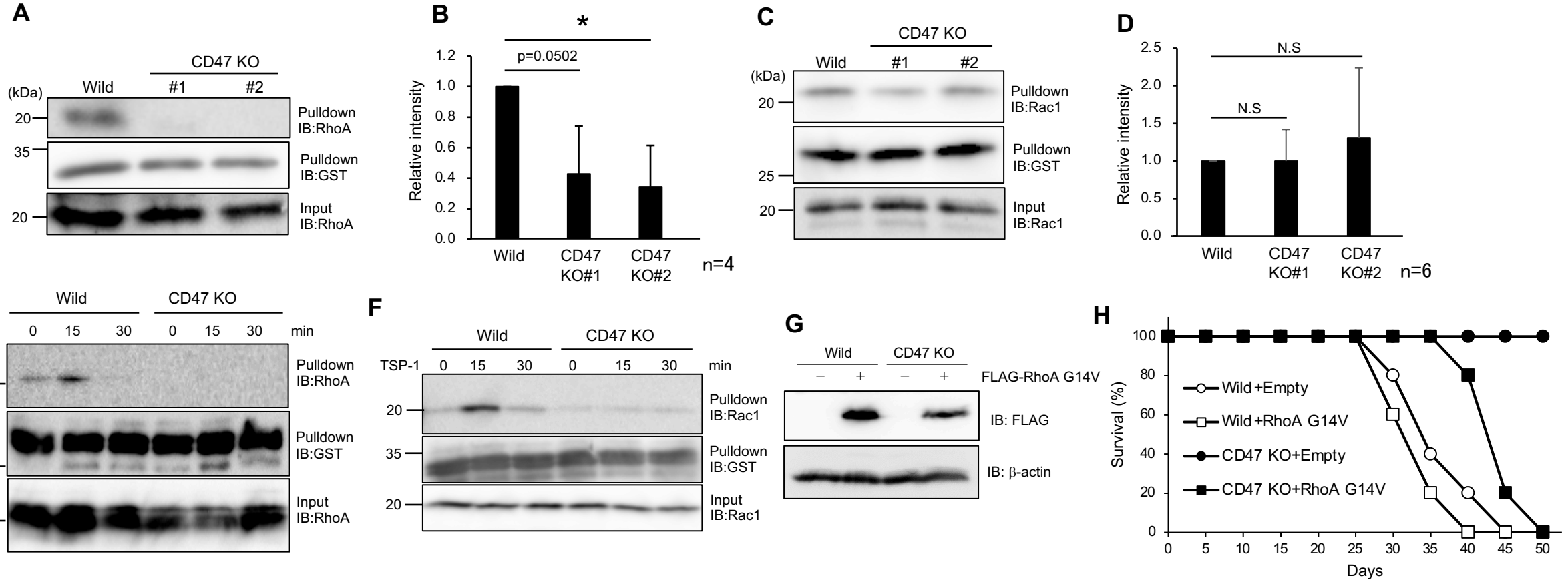
A
CD47 KO
Wild
#1
#2
(kDa)
20
35
20
Pulldown IB:RhoA
Pulldown IB:GST
Input IB:RhoA
B
*
p=0.0502
Relative intensity
1.2
1.0
0.8
0.6
0.4
0.2
0.0
Wild
CD47 KO#1
CD47 KO#2
n=4
C
CD47 KO
Wild
#1
#2
(kDa)
20
25
20
Pulldown IB:Rac1
Pulldown IB:GST
Input IB:Rac1
D
N.S
N.S
Relative intensity
2.5
2.0
1.5
1.0
0.5
0.0
Wild
CD47 KO#1
CD47 KO#2
n=6
E
Wild
CD47 KO
TSP-1
0
15
30
0
15
30
min
(kDa)
20
25
20
Pulldown IB:RhoA
Pulldown IB:GST
Input IB:RhoA
F
Wild
CD47 KO
TSP-1
0
15
30
0
15
30
min
20
35
20
Pulldown IB:Rac1
Pulldown IB:GST
Input IB:Rac1
G
Wild
CD47 KO
–
+
–
+
FLAG-RhoA G14V
IB: FLAG
IB: β-actin
H
Survival (%)
100
80
60
40
20
0
0
5
10
15
20
25
30
35
40
45
50
Days
Wild +Empty
Wild +RhoA G14V
CD47 KO+Empty
CD47 KO+RhoA G14V

Figure 5

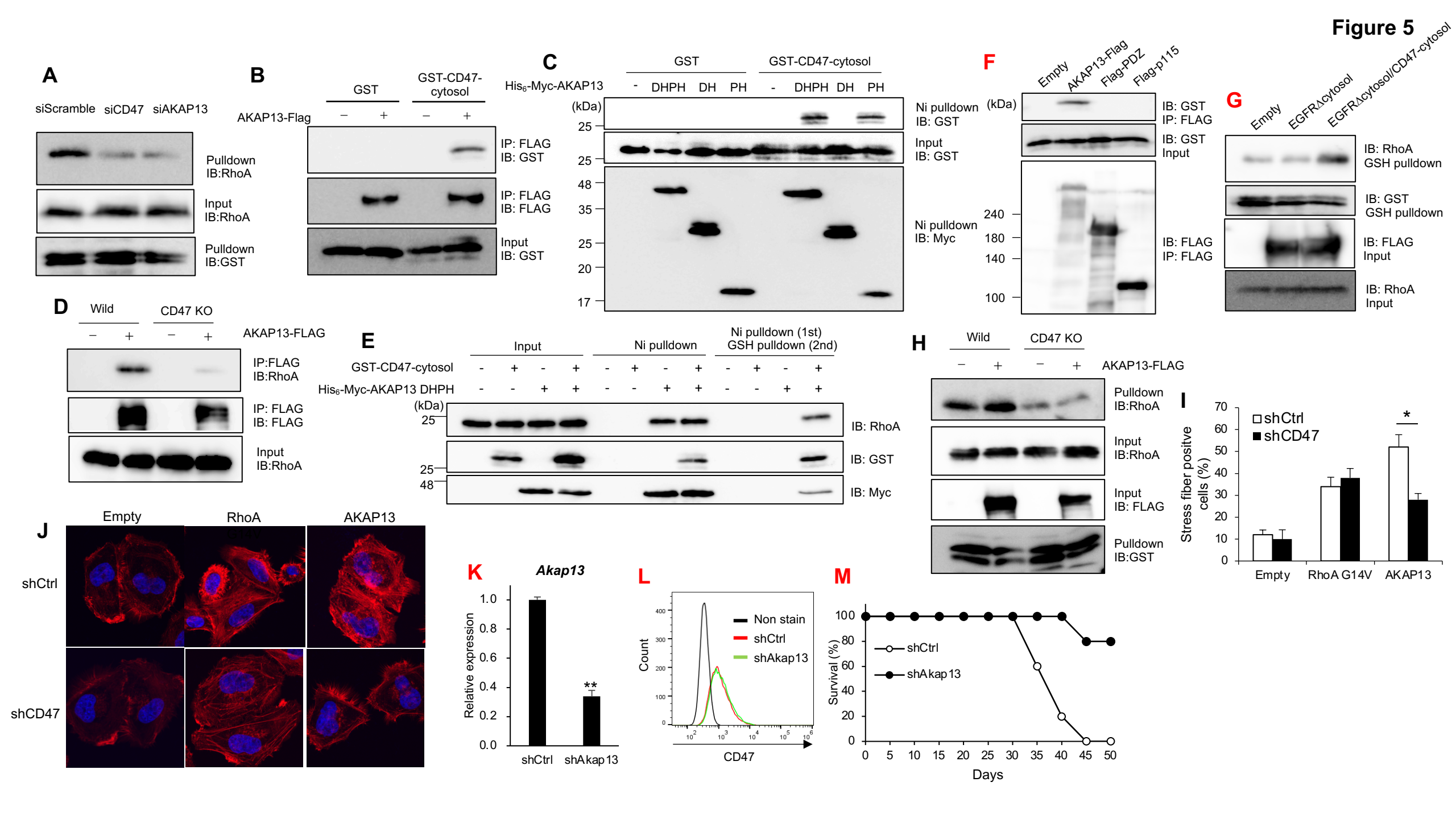
A
siScramble siCD47 siAKAP13
Pulldown IB:RhoA
Input IB:RhoA
Pulldown IB:GST
B
GST
GST-CD47-cytosol
AKAP13-Flag
IP: FLAG IB: GST
IP: FLAG IB: FLAG
Input IB: GST
C
GST
GST-CD47-cytosol
His6-Myc-AKAP13
DHPH DH PH
(kDa)
Ni pulldown IB: GST
Input IB: GST
Ni pulldown IB: Myc
F
Empty
AKAP13-Flag
Flag-PDZ
Flag-p115
IB: GST IP: FLAG
IB: GST Input
IB: FLAG IP: FLAG
G
Empty
EGFRΔcytosol
EGFRΔcytosol/CD47-cytosol
IB: RhoA GSH pulldown
IB: GST GSH pulldown
IB: FLAG Input
IB: RhoA Input
D
Wild
CD47 KO
AKAP13-FLAG
IP:FLAG IB:RhoA
IP: FLAG IB: FLAG
Input IB:RhoA
E
Input
Ni pulldown
Ni pulldown (1st) GSH pulldown (2nd)
GST-CD47-cytosol
His6-Myc-AKAP13 DHPH
IB: RhoA
IB: GST
IB: Myc
H
Wild
CD47 KO
AKAP13-FLAG
Pulldown IB:RhoA
Input IB:RhoA
Input IB: FLAG
Pulldown IB:GST
I
shCtrl
shCD47
Stress fiber positive cells (%)
Empty
RhoA G14V
AKAP13
J
Empty
RhoA
AKAP13
shCtrl
shCD47
K
Akap13
Relative expression
shCtrl
shAkap13
L
Non stain
shCtrl
shAkap13
Count
CD47
M
shCtrl
shAkap13
Survival (%)
Days